Global Change Biology (2002) **8,** 124–141

Modelling night-time ecosystem respiration by a constrained source optimization method

CHUN-TA LAI*, GABRIEL KATUL†, JOHN BUTNOR‡, DAVID ELLSWORTH§ and RAM OREN†

**Department of Biology, University of Utah, 257S. 1400E Salt Lake City, UT 84112-0840, USA; †Department of the Environment, Duke University, Durham NC 27708-0328, USA; ‡U.S.D.A. Forest Service, Southern Research Station, 3041 Cornwallis Road, Research Triangle Park, NC 27707, USA; § School of Natural Resources and the Environment, University of Michigan, Dana Building, 430 East University Avenue, Ann Arbor, MI 48109-1115, USA*

Abstract

One of the main challenges to quantifying ecosystem carbon budgets is properly quantifying the magnitude of night-time ecosystem respiration. Inverse Lagrangian dispersion analysis provides a promising approach to addressing such a problem when measured mean CO_2 concentration profiles and nocturnal velocity statistics are available. An inverse method, termed 'Constrained Source Optimization' or CSO, which couples a localized near-field theory (LNF) of turbulent dispersion to respiratory sources, is developed to estimate seasonal and annual components of ecosystem respiration. A key advantage to the proposed method is that the effects of variable leaf area density on flow statistics are explicitly resolved via higher-order closure principles. In CSO, the source distribution was computed after optimizing key physiological parameters to recover the measured mean concentration profile in a least-square fashion. The proposed method was field-tested using 1 year of 30-min mean CO_2 concentration and CO_2 flux measurements collected within a 17-year-old (in 1999) even-aged loblolly pine (*Pinus taeda* L.) stand in central North Carolina. Eddy-covariance flux measurements conditioned on large friction velocity, leaf-level porometry and forest-floor respiration chamber measurements were used to assess the performance of the CSO model. The CSO approach produced reasonable estimates of ecosystem respiration, which permits estimation of ecosystem gross primary production when combined with daytime net ecosystem exchange (NEE) measurements. We employed the CSO approach in modelling annual respiration of aboveground plant components ($c.\,214\,g\,C\,m^{-2}\,year^{-1}$) and forest floor ($c.\,989\,g\,C\,m^{-2}\,year^{-1}$) for estimating gross primary production ($c.\,1800\,g\,C\,m^{-2}\,year^{-1}$) with a NEE of $c.\,605\,g\,C\,m^{-2}\,year^{-1}$ for this pine forest ecosystem. We conclude that the CSO approach can utilise routine CO_2 concentration profile measurements to corroborate forest carbon balance estimates from eddy-covariance NEE and chamber-based component flux measurements.

Keywords: localized near field theory, inverse methods, ecosystem respiration, net ecosystem exchange, forest carbon budget

Received 13 November 2000; revised version received and accepted 11 April 2001

Introduction

Estimating monthly to annual ecosystem respiration (R_E) is essential in light of the pre-eminence of respiration in affecting net ecosystem CO_2 exchange (Baldocchi *et al*. 1997; Valentini *et al*. 2000). Long-term covariance measurements of net ecosystem exchange (NEE) are critical to estimating ecosystem carbon budgets, yet large errors arising from micrometeorological measurements of respiration under night-time conditions may corrupt NEE estimates (e.g. Wofsy *et al*. 1993; Baldocchi *et al*. 1996; Goulden *et al*. 1996; Moncrieff *et al*. 1996; Lindroth *et al*. 1998; Law *et al*. 1999a,b; Schmid *et al*. 2000; Valentini *et al*. 2000). Vertical subsidence, lack of

Correspondence: Chun-Ta Lai, tel. +801 581 8917, fax 801 581 4665, e-mail lai@biology.utah.edu

steadiness in mean atmospheric conditions and intermittent turbulent transport contribute to increase the 'de-coupling' between night-time net ecosystem respiration and the CO_2 flux above the canopy measured by covariance methods. Instrument limitations, such as separation between sensors that are assumed to measure the same parcel of air, attenuation of fluctuation in the tube, volume averaging by anemometers, and finite sampling periods that may be too short to resolve all the eddy sizes, further compound the random and systematic errors in night-time flux measurements (Kaimal & Gaynor 1991; de Bruin *et al*. 1993; Kaimal & Finnigan 1994; Leuning & Judd 1996; Moncrieff *et al*. 1996; Massman 2000).

An alternative approach to estimating R_E is to utilize a functional relationship between CO_2 sources, $S(t,z)$, or fluxes, $F(t,z)$, and a relatively simple quantity to measure such as mean CO_2 concentration, $C(t,z)$, within the canopy volume, where t is time and z is the height from the forest floor. This approach has the added benefit of permitting detailed partitioning of $S(t,z)$ between different canopy levels and between the vegetation and the forest floor efflux $F(t,0)$.

Early research efforts derive these functional relationships by assuming $F(t,z)$ is related to dC/dz via an effective turbulent diffusivity (K-Theory). Over the past 30 years, theoretical developments and many laboratory and field experiments have demonstrated that scalar and momentum fluxes within many canopies do not obey K-Theory (e.g. Deardorff 1972, 1978; Corrsin 1974; Shaw 1977; Sreenivasan *et al*. 1982; Denmead & Bradley 1985; Finnigan 1985; Raupach 1988; Wilson 1989). To alleviate K-Theory limitations, other theoretical and practical methods were developed without resorting to a local eddy diffusivity approximation (e.g. Raupach 1988, 1989a,1b; Katul & Albertson 1999; Katul *et al*. 2000a; Siqueira *et al*. 2000).

This study builds on these recent advances to develop a method capable of inferring $F(t,0)$ and $S(t,z)$ from measured $C(t,z)$ for long-term estimation of night-time R_E. To successfully reproduce $F(t,z)$ from measured $C(t,z)$, the following conditions must be satisfied: (i) accurate description of the flow statistics inside the canopy for stable atmospheric conditions, (ii) explicit accounting of storage fluxes within the canopy volume, and (iii) constraining the estimation of $S(t,z)$ so as to minimize the effect of inherent measurement and sampling errors in $C(t,z)$ on the computed $S(t,z)$. The objective of this study is to develop a method, termed 'Constrained Source Optimization' or CSO, capable of reproducing night-time ecosystem fluxes and R_E components from measured $C(t,z)$. The method is tested using 1 year of 30-minute measured mean CO_2 concentration profiles $C(t,z)$ collected within a 17-year-old (in 1999) even-aged loblolly pine (*Pinus taeda* L.) stand at the Duke Forest. Rather than propose a *replacement* method to night-time covariance, chamber-scale measurements, or other established respiration measurement methods, we propose here a *complementary* method that can independently assess monthly to annual R_E estimates from routinely measured $C(t,z)$. Such an assessment is essential because forest floor respiration is a major component of forest gross primary production (Baldocchi *et al*. 1997; Law *et al*. 1999b; Valentini *et al*. 2000).

Theory

In order to estimate R_E, both the source $S(t,z)$ in the canopy and the forest floor CO_2 flux $F(t,0)$ are required because

$$R_E = \int_0^h S(t,z)\,dz + F(t,0) \tag{1}$$

where h is the mean canopy height. Measured $C(t,z)$ can be related to $S(t,z)$ or $F(t,z)$ using the time and horizontally averaged one-dimensional continuity equation for a planar homogeneous flow,

$$\frac{\partial C(t,z)}{\partial t} = -\frac{\partial F(t,z)}{\partial z} + S(t,z) \tag{2}$$

Equation 2 has two unknowns, $S(t,z)$ and $F(t,z)$, and requires one additional prognostic equation to solve for R_E. One approach to establish this requisite equation is to consider the interdependency between $S(t,z)$ and $C(t,z)$ via Lagrangian dispersion theory, which is considered next.

Lagrangian Dispersion Theory

The localized near-field theory (LNF) proposed by Raupach (1989a,b) can be used to describe a canonical relationship between $S(t,z)$ and $C(t,z)$. According to Raupach (1989a,b), $C(t,z)$ can be decomposed into far-field (C_f) and near-field (C_n) concentrations, with the near-field concentration at z given by

$$C_n(z) = \sum_0^h \frac{S(z_o)}{\sigma_w(z_o)} \left\{ k_n\left[\frac{z - z_o}{\sigma_w(z_o)T_L(z_o)}\right] + k_n\left[\frac{z + z_o}{\sigma_w(z_o)T_L(z_o)}\right]\right\} \Delta z_o \tag{3}$$

where Δz_o is the vertical interval between source locations, $\sigma_w(z)$ is the standard deviation of the vertical velocity at height z, $k_n(\zeta) = -0.3989 \ln\left(1 - e^{-|\zeta|}\right) - 0.15623e^{-|\zeta|}$ is a near-field kernel function, and ζ is a dummy variable. This analytical approximation to the kernel and resulting errors ($< 6\%$) are discussed in Raupach (1989a,b, 1998) and Gu (1998). Given a reference concentration

(C_r) at $z/h > 1$, the diffusive, far-field concentration (C_f) can be expressed as:

$$C_f(z) = C_r(z_R) - C_n(z_R) + \sum_{z}^{z_R} \frac{F(z)}{K_f(z)} \Delta z \qquad (4)$$

where Z_R is a reference (or measurement) height, and

$$K_f(z) = \sigma_w^2(z) T_L(z) \qquad (5)$$

is the far-field eddy diffusivity in a steady, homogeneous turbulent flow, and T_L is the Lagrangian integral time scale. We emphasize here that while steady-state diffusion is assumed in equations 3 to 5, the mass conservation equation in equation 2 is non-steady.

Many laboratory and field experiments demonstrated that LNF is a significant improvement over gradient-diffusion theory (Raupach *et al*. 1992; Denmead & Raupach 1993; Denmead 1995; Katul *et al*. 1997a; Massman & Weil 1999; Leuning 2000; Leuning *et al*. 2000; Siqueira *et al*. 2000). Therefore, LNF was used to describe the scalar transport in the CSO. Other models equally suitable to CSO include the Eulerian closure approach of Katul & Albertson (1999) and Katul *et al*. (2000a), the Hybrid approach of Siqueira *et al*. (2000), or the recent revision to LNF by Warland & Thurtell (2000).

For LNF, given T_L and σ_w, equations 3–5 provide the independent formulation necessary to relate C to S and F, thereby 'closing' equation 2 and, in principle, permitting night-time R_E to be computed from measurements of C. As discussed in Katul *et al*. (1997a, 2000a), the conventional inverse LNF approach is not sufficiently 'robust' to measurement errors because, in practice, the difference between the number of source layers and the number of concentration measurement layers is typically small. Naturally, such a small difference implies limited degrees of freedom (usually ≤ 3) in the estimation of S from C. We describe next the CSO, which is a variant on Raupach's (1989b) inversion to generate the desirable robustness in the inference of S from C.

Constrained Source Optimization (CSO) method

As described by Raupach (1989b), it is possible to solve for the source S and the flux F from the mean CO_2 concentration profile C by the so-called 'inverse' approach. In this method, the canopy is first divided into m' source layers, where $m' \leq m$, and m is the number of levels where $C(z_i)$ are measured ($i = 1, 2 \cdots m$). The challenge is to determine the optimum source distribution $S(z_j)$ ($j = 1, 2 \cdots m'$) that best recovers the measured $C(z_j)$ using LNF and prescribed flow statistics (e.g. $\sigma_w(z)$, T_L). As discussed in Katul *et al*. (1997a) and Siqueira *et al*. (2000), this inverse procedure is very sensitive to the choice of m' and m, as well as to the random measurement errors in $C(z_i)$. With $m - m' < 3$ for most field studies, spurious sources and sinks may be produced from measurements and sampling errors in C (see Katul *et al*. 2000a; Siqueira *et al*. 2000). To minimize such sensitivity and increase the degrees of freedom in the estimation of S from C, an alternative approach that utilizes known canopy physiological properties and attributes is proposed.

Total above-ground plant respiration ($= \int_0^h S(t,z)dz$) can be decomposed into woody tissue and foliage respiration (F_f). According to Law *et al*. (1999b), wood respiration accounted for about 6% of total R_E in a ponderosa pine ecosystem, while foliage respiration accounted for about 18%, despite the relatively low leaf area density in that forest. In our region, atmospheric demand for vapour is lower than that in the Oregon ponderosa pine ecosystem, thus requiring less woody water transport system per unit of leaf area (Oren *et al*. 1986). Therefore, we assumed the contribution of wood respiration would be even less important relative to the foliage respiration in comparison to the ponderosa pine ecosystem. Consequently, the contribution of woody components to above-ground ecosystem respiration was not explicitly separated from foliage in this study. In a nearby stand of similar characteristics, the contribution of woody surface area to plant area density was 18% (Pataki *et al*. 1998). This is an underestimate of the total woody surface area in the stand and hence the actual amount of respiring woody biomass. This was partially compensated for in the calculations of respiration by assuming that the entire plant area density was composed of foliage with its characteristically higher respiration rates.

With this simplification, a first order estimate of the vertical distribution of S can be specified *a priori* as

$$S(z) = a(z) R_d(z) \qquad (6)$$

where $a(z)$ is the plant area density and R_d is the dark respiration per unit plant area modelled after Collatz *et al*. (1991) as

$$R_d(z) = \alpha V_{cmax}(z) \qquad (7)$$

where α is, in our approach, an unknown constant and $V_{cmax}(z)$ is the maximum catalytic capacity of Rubisco per unit leaf area. The scaling between R_d and V_{cmax} assumes that respiration is mainly a function of enzyme turnover associated with the maintenance of photosynthetic enzymes, principally ribulose 1,5-bisphosphate carboxylase as represented by V_{cmax}. Naturally, other models for R_d can be readily implemented in such a framework. Both V_{cmax} and α are temperature-dependent (Campbell & Norman 1998). Typical α values at 25 °C are assumed between 0.011 and 0.015 (Farquhar *et al*. 1980; Collatz *et al*. 1991). Here, the temperature dependency of V_{cmax} can be calculated from

$$V_{c\,\max}(T_a) = \frac{V_{c\,\max,\,25}\exp[a_1(T_a - 25)]}{1 + \exp[a_2(T_a - 55)]} \qquad (8)$$

where, $V_{cmax,25}$ is the maximum catalytic rate of Rubisco at 25 °C, T_a is the air temperature (which approximates the plant tissue temperature during night time), and a_1 and a_2 are species-specific coefficients as discussed by Lai *et al*. (2000a), which were reported, respectively, as 0.051 and 0.205 for overstorey pine ($0.4 < z/h < 1$) and as 0.088 and 0.290 for the understorey hardwood ($0 < z/h < 0.4$). Long-term averaged values of $V_{cmax,25} = 59$ μmol m^{-2} s^{-1} for pines and 30 μmol m^{-2} s^{-1} for the hardwood species are used, as discussed by Ellsworth (1999), DeLucia & Thomas (2000) and Naumburg & Ellsworth (2000).

We define the constrained source optimization (CSO) method as the combination of α and forest floor flux $F(t,0)$ used in equations 2–5 to recover the measured $C(z_i)$ in a least-square manner (e.g. optimized) every 30 min. When compared to Raupach's (1989b) inverse method, this approach offers several advantages for night-time source calculations:

1. The proposed CSO modelling approach prescribed and constrained $S(z)$ by our understanding of the vertical distribution of $a(z)$ and $V_{cmax}(z)$, both measured quantities, but allowing determination of ecosystem respiratory fluxes $F(t,z)$ via optimizing α and $F(t,0)$ to reproduce the CO_2 concentration field for a wide range of stable atmospheric conditions. In essence, the number of unknowns was greatly reduced to $m' = 2$. The redundancy in the proposed optimization is greater (typically, $m - 2$ varies from 6 to 8) when compared to Raupach's (1989b) method ($m - m' \leq 3$ for nearly all LNF field studies conducted thus far). Hence, with such redundancy, S and $F(t,0)$ are no longer 'hypersensitive' to random measurement and sampling errors in $C(z_i)$.
2. Because the number of parameters is small (only α and $F(t,0)$), a global optimization method can be efficiently implemented. This global search can be readily constrained by the maximum range in α and $F(t,0)$ from literature values. For example, a global search with α between 0.001 and 0.05, and $F(t,0)$ between 0 and 30 μmol $m^{-2}s^{-1}$, should yield reasonable sources and forest floor fluxes observed in majority of field experiments.
3. The method takes advantage of the measured plant area density $a(z,t)$ dynamics when computing the canopy sources. Plant area density distribution and dynamics are not well utilized in the LNF approach of Raupach (1989a, b).

The velocity statistics and integral time scale

Ideally, the measured $\sigma_w(z)$ should be used in equation 3 and 5. However, these measurements are rarely available on a routine basis on monthly to annual time scales. Higher-order Eulerian closure models provide an alternative to routine estimation of $\sigma_w(z)$ provided that they can be validated via short intensive field campaigns. A key advantage to such a model framework is its ability to map variability in $a(z,t)$ to variability in $\sigma_w(z,t)$.

In order to model the σ_w within the canopy volume, we chose the second-order closure approach by Wilson & Shaw (1977) (hereafter referred to as WS77; see Appendix 1 for details). The ability of this model to reproduce measured σ_w inside forested canopies was found to be comparable to third-order closure schemes (Katul & Albertson 1998) and other multiscale second order closure schemes (Katul & Chang 1999). Furthermore, obtaining the numerical solution to the WS77 closure equations does not require complex numerical integration algorithms, at least when compared to the recently proposed closure model of Ayotte *et al*. (1999). Although the WS77 assumes neutral atmospheric conditions, the effects of atmospheric stability can be indirectly accounted for by revising the upper boundary conditions to evolve with h/L, where L is the Obukhov length typically measured at a reference height above the canopy–atmosphere interface.

With regards to the integral time scale, Raupach (1989a,b) suggested that $\frac{T_L u_*}{h} \approx 0.3$ as a constant within the canopy volume, where u_* is the friction velocity. While the 0.3 value appears reasonable for unstable and near-neutral atmospheric stability conditions (Katul *et al*. 1997a), little evidence is available to support such a constant value for stable conditions. In this study, we assess the sensitivity of the R_E calculation to three different formulation of $\frac{T_L u_*}{h}$:

$$\frac{T_L u_*}{h} = \begin{cases} 0.3 \\ \phi_1\left(\dfrac{h}{L}\right) \\ \phi_2\left(\dfrac{h}{L}, \dfrac{z}{h}\right) \end{cases} \qquad (9)$$

where, ϕ_1 and ϕ_2 are determined from detailed Eulerian vertical velocity integral time-scale measurements (T_w) and assuming $T_w \approx \frac{3}{4} T_L$ (Tennekes & Lumley 1972). Estimates of T_w can be derived from the autocorrelation function $\rho_w(\tau)$ of the vertical velocity fluctuations w':

$$T_w = \int_0^\infty \rho_w(\tau) d\tau, \text{ and}$$

$$\rho_w(\tau) = \frac{1}{\sigma_w^2}\overline{w'(t)w'(t+\tau)} \qquad (10)$$

where overbar represents time averaging (i.e. $\overline{w'} = 0$), and τ is the time lag. The above integration is commonly terminated at the first zero crossing of $\rho_w(\tau)$. If such a crossing is not well defined (as may be the case for some

very stable runs), the integration is terminated at the first τ for which $\rho_w(\tau)$ is no longer statistically different from zero at the 99% probability level. This probability limit on $\rho_w(\tau)$ can be determined from Salas *et al*. (1984):

$$\rho_{99\%}(\tau) = \frac{-1 \pm 2.326\sqrt{N - \tau f_s - 1}}{N - \tau f_s} \qquad (11)$$

where N is the number of sample points, and f_s is the sampling frequency (e.g. $N = 18000$ for $f_s = 10$ Hz and a 30 min sampling duration). Hence, for consistency, the integration in equation 10 is terminated when $\rho_w(\tau) \approx \rho_{99\%}(\tau)$ (rather than zero) for all runs.

Study site and measurements

Study site

The measurements are conducted at the Blackwood Division of Duke Forest in Orange County, near Durham, NC, USA (36°2′ N, 79°8′ W) as part of the AmeriFlux long-term CO_2 flux monitoring initiative (Kaiser 1998). The site is a uniformly planted loblolly pine (*Pinus taeda* L.) forest that extends 300–600 m in the east–west direction and 1000 m in the north–south direction. The mean canopy height was 14 m ($\pm$ 0.5 m) at the end of 1998. The change of topographic slope is small (< 5%) so that the turbulent transport is not confounded by terrain (Kaimal & Finnigan 1994). All the measurements and parameterizations in this study were from the tower in ambient conditions.

Eddy covariance flux measurements

The CO_2, latent and sensible heat fluxes above the canopy were measured by a conventional covariance system comprising of a Licor-6262 CO_2/H_2O infrared gas analyser (Li-Cor Inc., Lincoln, NE, USA) and a Campbell Scientific sonic anemometer (CSAT3, Campbell Scientific Inc., Logan, UT, USA). The sonic anemometer was positioned just above the canopy ($z = 15.5$ m). The infrared gas analyser was housed in an enclosure on the tower 4.5 m below the inlet cup, which was co-located with the anemometer. The sampling flow rate for the gas analyser is 9 L min^{-1}, sufficient to maintain turbulent flows in the tubing. A krypton hygrometer (KH2O, Campbell Scientific) was positioned with the anemometer to assess the magnitude of the tube attenuation and time lag between vertical velocity and scalar concentration fluctuations as discussed in Katul *et al*. (1997a, 2000a).

The flux measurements were sampled at 10 Hz using a Campbell Scientific 21X data logger with all digitized signals transferred to a portable computer via an optically isolated RS232 interface for future processing. Details about the processing and corrections to these high frequency measurements are described in Katul *et al*. (1997a,b).

Mean CO_2 and water vapour concentration profiles within the canopy

Another LiCor-6262 gas analyser was used to measure CO_2 and water vapour concentration profiles at 10 levels ($z_i = 0.1$, 0.5, 1.5, 3.5, 5.5, 7.5, 9.5, 11.5, 13.5 and 15.5 m, i.e. $m = 10$). This profiling system includes a multiport gas sampling manifold to sample each level for 1 min (45 s sampling and 15 s purging) at the beginning, the middle, and the end of 30-minute sampling duration. In 1999, the experiment resulted in 4850 30-minutes night-time runs for which simultaneous CO_2 concentration and flux measurements were available between 2030 and 0430 EST.

Other meteorological and biological variables

In addition to the covariance flux measurements above the canopy, a HMP35C Ta/RH probe (Campbell Scientific) was also positioned at $z = 15.5$ m to measure mean air temperature (T_a) and mean relative humidity. A nonlinear thermistor (Campbell Scientific) was positioned at 15 cm below the forest floor, adjacent to the tower, to measure mean soil temperature (T_s). All the meteorological variables were sampled at 1 s and averaged every 30 min using a 21X Campbell Scientific data logger. A total of 45 leaf-level CO_2 assimilation (A_{net}) responses to CO_2 supply ($A_{net} - C_i$ curves), conducted within a 14-month period between 1998 and 1999, were also used to estimate V_{cmax} using the least-square regression procedure described by Wullschleger (1993) and Ellsworth (2000), where C_i is the leaf internal CO_2 mole fraction. Further details about the gas exchange measurements and sampling methodology can be found in Ellsworth (1999, 2000) and Katul *et al*. (2000b).

Plant area density

The vertical variation of the leaf area plus branches was measured by gap fraction techniques as described by Norman & Welles (1983). A pair of optical sensors with hemispherical lenses (LAI-2000, Li-Cor) was used for canopy light transmittance measurements from which gap fraction and plant area densities were calculated. The measurements were made at 1 m intervals from the top of the canopy to 1 m above the ground to produce the vertical profile in plant area index (PAI). PAI measurements were made routinely during the experimental periods, from the same tower used for measuring flow statistics, CO_2 concentration and covariance

measurements. For time increments between these measurements, the PAI values were linearly interpolated. The vertical foliage distributions $a(z)$ were generated using three canonical PAI profiles representing winter (December to April), summer (June to October) and transition periods (May and November).

Soil respiration measurements

Soil respiration $F(t,0)$ was measured with a custom designed, chamber based system – Automated Carbon Efflux System (ACES) – based on principles used in Maier & Kress (2000). ACES is a multiport, dynamic gas sampling system that utilizes an open flow-through design to measure carbon dioxide fluxes from the forest floor. Each chamber was equipped with a pressure equilibration port, ensuring that the chamber pressure was held near ambient (Fang & Moncrieff 1996). Fifteen soil chambers (25 cm diameter, 10 cm height, 4909 cm^3) were measured sequentially using a single infrared gas analyser (EGM-3, PP Systems Inc., Haverhill, MA, USA) integrated into the system. Each chamber was sampled for 10 minutes to ensure steady state conditions, and a value of $F(t,0)$ was recorded on the tenth minute of the cycle. Nine complete runs (135 measures) were recorded every day. When not being actively sampled, all chambers were continuously supplied with ambient air to prevent CO_2 build-up. Data were collected continuously from April to May 2000. To lessen chamber induced impacts on the soil surface, chambers were moved twice a week between two fixed sample points.

Velocity statistics measurements for testing WS77

To estimate ϕ_1 and ϕ_2 in equation 9 and test the WS77 model performance for stable atmospheric conditions, an intensive field experiment was conducted. The three velocity components and virtual potential temperature inside the canopy were measured at eight levels ($z = 1.3$, 2.9, 4.8, 6.5, 8.5, 10.7, 12.1, 15.5 m) from 23–30 August 1999 with a vertical array of eight CSAT3 sonic anemometers. Each sonic anemometer was anchored on a horizontal bar extending 1 m away from the walkup tower. The sampling frequency was 10 Hz for all sonic anemometers. All analogue signals were digitized by a Campbell Scientific CR-9000 data logger and transferred to a laptop computer for future processing. This experiment was performed at the same flux tower site used to measure plant area density, the long-term scalar fluxes and concentration profiles thereby permitting to assess the WS77 performance of reproducing $\sigma_w(z)$ using the locally measured $a(z)$. The velocity statistics were collected over a wide range of atmospheric stability conditions; however, here we focus only on stable atmospheric conditions.

Results and discussion

We assessed the performance of the CSO by (i) comparing the predicted night-time ecosystem fluxes with eddy covariance measurements collected at $z/h = 1.1$ for high u_* ($> 0.15\,m\,s^{-1}$), (ii) verifying whether the optimized α is bounded by leaf-level measurements, and (iii) evaluating the similarity of forest floor respiration–soil temperature response function computed with the CSO to functions derived from chamber measurements. Finally, the seasonal dynamics of R_E and its components, as modelled by the CSO, are discussed in the context of the annual carbon budget and gross primary production (GPP) of this forested ecosystem. Before presenting the modelled R_E results, we consider the estimation of the flow statistics inside the canopy that are essential to drive the CSO method.

Velocity statistics for nocturnal conditions

To model night-time R_E using LNF, the velocity statistics σ_w and T_L are required. Figure 1 shows the measured $\frac{T_L u_*}{h}$ and σ_w/u_* at $z/h = 1.1$ for a wide range of stable atmospheric conditions. Here, T_L is derived from the Eulerian integral time scale (T_w) described in equation 10. The apparent increase of σ_w/u_* from the value of 1.1 for large h/L is attributed to the fact that random errors tend to increase σ_w but decrease u_* over very stable conditions. Hence, we assumed that $\sigma_w/u_* = 1.1$ for the entire h/L range. This is consistent with the findings of Leuning (2000) that thermal stratification has little effect on σ_w.

While the normalized σ_w remains nearly constant (*c.* 1.1), the $\frac{T_L u_*}{h}$ is greatly reduced with increasing stability (a reduction factor of 10 for two decades of h/L). Based on these field observations, $\frac{T_L u_*}{h}$ was made to vary with h/L. This variation is also consistent with findings in a recent study by Leuning (2000) in which the LNF performance was significantly improved when T_L was corrected based on atmospheric stability. To quantify the stability effects on T_L, we fitted an exponential curve $f_\phi(h/L)$ to the measurements in Fig. 1. The fitted curve was used to compute T_L based on measured h/L at $z/h = 1.1$. The above analysis completes the description of the upper boundary condition for the canopy volume in order to generate the flow statistics for LNF.

The within-canopy vertical variation of σ_w and T_L are considered using the intensive velocity statistics measurements collected inside the canopy. Figure 2 shows the normalized ensemble σ_w and T_L profiles inside the canopy for nocturnal conditions collected in August 1999. Although WS77 does not explicitly account for density gradients, it can reproduce night-time σ_w reasonably well

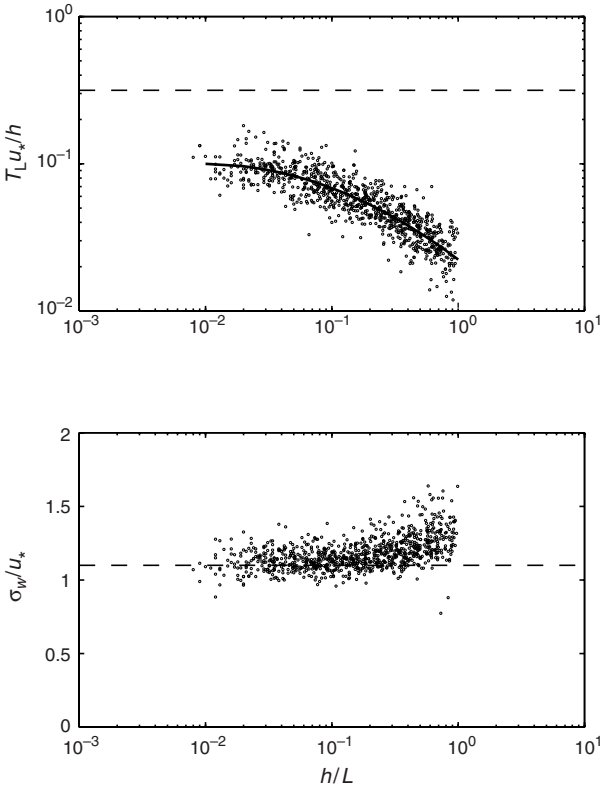

Fig. 1 Normalized T_L (top) and σ_w (bottom) measured (○) at $z/h = 1.1$ for different stable conditions. Solid line is the fitted curve used in the CSO calculation. Dashed lines are the values for near-neutral conditions within the canopy sublayer.

if the empirical constant in the characteristic length scale is varied from its neutral value to match best the measured mean wind field (see Appendix 1). The σ_w profile from WS77, obtained with the revised length scale constant, is used in the LNF calculation for the entire study period.

While the vertical variation in T_L cannot be directly measured, it may be inferred from measured T_w shown in Fig. 2. The fact that the measured T_w profile is not constant within the canopy volume motivated us to consider three possible scenarios for the space-time variation in T_L, shown in Fig. 3, and described below in the following three cases.

1. $\frac{T_L u_*}{h} = 0.3$, constant throughout the canopy without any stability correction.
2. $\frac{T_L u_*}{h} = f_\phi$ where $f_\phi = \phi_1\left(\frac{h}{L}\right) = \exp(-0.0695x^2 - 0.6454x - 3.8516)$, $x = \ln(\frac{h}{L})$, and L is calculated from the sensible heat and friction velocity measurements collected at the canopy top. Here, T_L is also assumed constant within the canopy but varies with atmospheric stability at $z/h = 1.1$.

Finally, the case for which T_L varies with both atmospheric stability h/L and z/h as derived from T_w measurements is also shown. This case can be approximated by

3. $$\frac{T_L u_*}{h} = \phi_2\left(\frac{h}{L}, \frac{z}{h}\right) = f_\phi - 0.155 \times (z_c - 1),$$

where

$$\begin{cases} z_c = 0.4 & \text{if } z/h < 0.4 \\ z_c = z/h & \text{if } z/h \geq 0.4 \end{cases}.$$

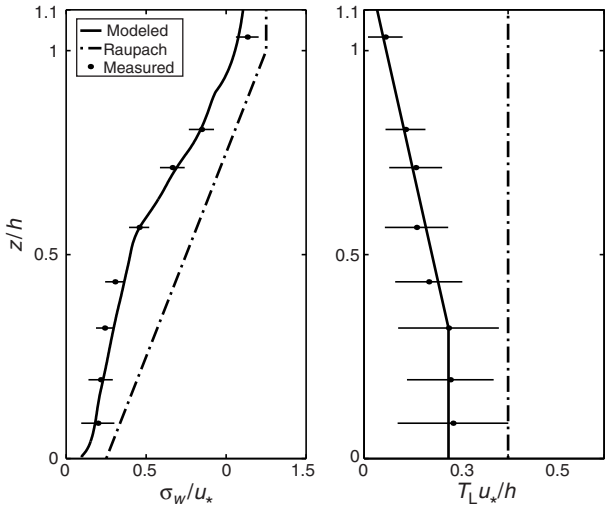

Fig. 2 Comparison between ensemble averages of within canopy T_L (right) and σ_w (left) profiles measured in August 1999 and modelled based on WS77. For reference, the profiles suggested by Raupach (1989a,b) are also shown.

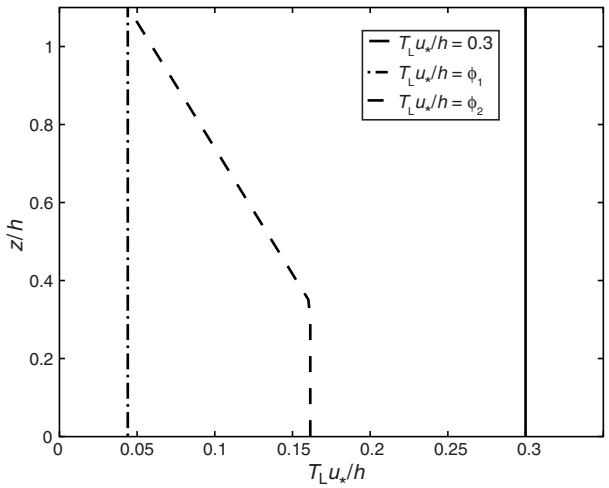

Fig. 3 Three plausible T_L profiles tested in the CSO approach. For the $T_L u_*/h = f_\phi(\phi_1, \phi_2)$, we present as a sample $T_L u_*/h = 0.044$ at $z/h = 1.1$ derived from the long-term mean value in Fig. 2.

Again, we emphasize that this profile assumes $T_w \approx \frac{3}{4}T_L$ and is based on the measurements shown in Fig. 2. From the analysis in Appendix 2, we found that case 2 provides the most reasonable result, although the differences between cases 2 and 3 was at most 10%. For the remaining discussion the T_L profile of case 2 was used.

Model optimization

Given the modelled velocity field and assuming some α and $F(t,0)$, the night-time CO_2 concentration profile can be computed using equations 3–5. The α and $F(t,0)$ are then allowed to vary until the root-mean square error (RMSE) between predicted and measured CO_2 concentrations at 9 levels is minimized.

The optimization was conducted for each 30 min run with

1. $\frac{h}{L} > 0$, (i.e. stable atmospheric conditions)
2. measured $F(t,h) > 0$ (ecosystem respiration exceeds photosynthesis), and
3. RMSE $< 10\,\mu$ mol mol^{-1} (i.e. LNF reproduces well the measured concentration).

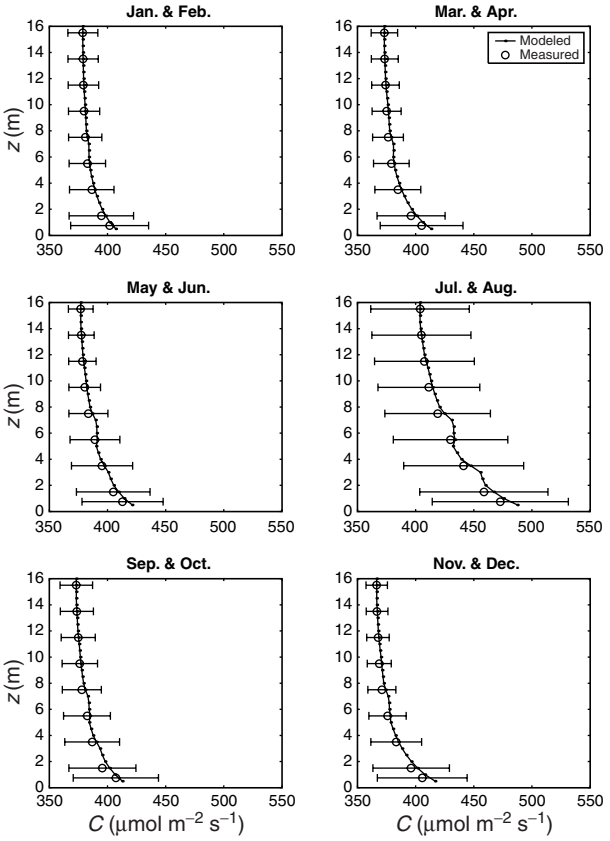

Fig. 4 Comparison between measured and CSO modelled ensemble averaged $C(t,z)$ within the canopy. The comparison is reported for data combined over two consecutive months, thereby allowing demonstrating seasonal variations.

These three criteria resulted in 2418 30-minute evening runs between 2030 and 0430. The resulting optimized concentration profiles are shown in Fig. 4 after ensemble averaging every 2 months (to illustrate seasonal patterns). As evidenced from Fig. 4, the C profiles computed with CSO from optimized α and $F(t,0)$ are in good agreements with the ensemble-averaged C measurements.

Model validation

To assess how well CSO reproduced R_E, we consider the following:

1. Comparisons between predicted and measured ensemble of $F(t,h)$ for $u_* > 0.15\,\mathrm{m\,s^{-1}}$. The latter u_* condition is used to ensure that the measured $F(t,h)$ reliably represents net ecosystem exchange (NEE) (Falge *et al*. 2000).
2. A comparison between modelled forest-floor–temperature function and chamber-measured response functions.
3. Whether the optimized α value is bounded by the porometry chamber measurements of leaf R_d.
4. On longer time scales, whether the modelled ratio of forest floor to total ecosystem respiration is consistent with independently established estimates derived from biomass increment and other ecological measurements.

Comparisons between modelled and covariance measured $F(t,h)$

A number of previous studies have found that during night-time conditions, the NEE measurements by eddy covariance may not be reliable (e.g. Wofsy *et al*. 1993; Hollinger *et al*. 1994; Black *et al*. 1996; Goulden *et al*. 1996; Baldocchi *et al*. 1997; Lavigne *et al*. 1997; Law *et al*. 1999a). For example, when eddy covariance measurements were compared to the chamber-estimated soil surface efflux in a ponderosa pine forest in Oregon, the underestimation was as large as 50% (Law *et al*. 1999b). On the other hand, other field experiments did not find such discrepancies (Grace *et al*. 1996). Uncertainty in these comparisons may be complicated by the storage flux (F_{st}), which is given by

$$F_{st} = \int_0^h \frac{\partial C}{\partial t} dz \qquad (12)$$

Greco & Baldocchi (1996) reported that F_{st} averages to near zero on a daily basis, although it may be significant

in the evenings. Previous measurements at this site also showed that F_{st} averages to zero on a daily basis but is significant during sunrise and sunset periods (Lai *et al.* 2000b). For this study, F_{st} was calculated using measured mean CO_2 concentration every 30 min for the selected night-time runs (from 2030 to 0430) and was included for reference in the comparison between measured and modelled ecosystem respiration.

Upon integrating equation 2 with respect to z, we obtain

$$\int_0^h \frac{\partial C(t,z)}{\partial t} dz + F(t,h) = F(t,0) + \int_0^h S(t,z) dz, \qquad (13)$$

in equation 13, the left-hand side represents the measured ecosystem respiration and the right-hand side represents the so-called 'biotic' fluxes. To illustrate the seasonal variation in these components, we report the ensemble averages of measured $F_{st} + F(t,h)$ and CSO-modelled $F(t,0) + \int_0^h S(t,z)\, dz$ every 2 months for evening runs between 2030 and 0430 in Fig. 5. For $u_* > 0.15\,\mathrm{m\,s^{-1}}$ (a threshold used by several investigators including Goulden *et al.* 1996 and Clark *et al.* 1999), our model calculation agrees closely with measured $F_{st} + F(t,h)$ for the winter periods. However, modelled $F(t,0) + \int_0^h S(t,z)dz$ tends to be greater than measured $F_{st} + F(t,h)$ by up to 30% in the summer. This discrepancy may be an artifact of the modelled time scale (T_L), or an indication of missing fluxes which are not well captured by either eddy covariance system or the profiling system used to estimate the storage flux. Generally F_{st} are small except for summer months, when mean CO_2 concentration near the forest floor ($z < 10$ cm) is large and dynamic. We emphasize that both measured $F(t,h)$ and F_{st} suffer from random and sampling errors.

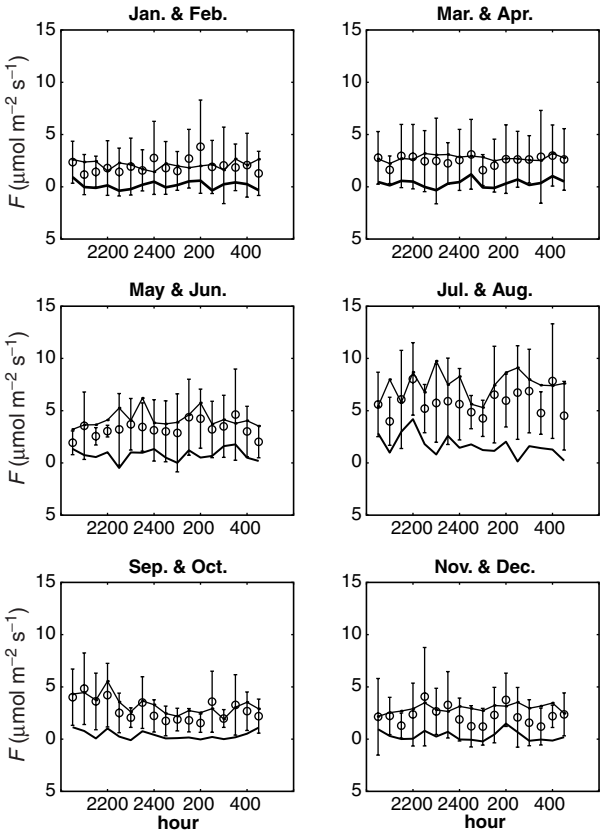

Fig. 5 Comparison between measured (○ with one standard deviation) and CSO modelled (solid line) $F(t,h)$. The measured $F_{st}(t)$ (thick solid line) is also shown for reference.

Optimized forest-floor respiration

In order to compare the CSO model results with other studies and chamber measurements available at this site, the CSO-optimized forest floor respiration are presented as a function of soil temperature (e.g. Raich & Schlesinger 1992; Wofsy *et al.* 1993; Hollinger *et al.* 1994; Lloyd & Taylor 1994; Fan *et al.* 1995; Lindroth *et al.* 1998; Law *et al.* 1999a,b). Regressing the CSO modelled $F(t,0)$ with soil temperature (T_s) measured at 15 cm below the ground surface resulted in

$$F(t,0) = 1.198 \exp(0.054\mathrm{Ts}) \qquad (14)$$

This regression was performed with bin-averaged respiration values for 5 °C increments of T_s (Fig. 6a). Figure 6(b) shows the comparison between this function and functional relationship derived from the ACES chamber measurements, along with functions reported in other studies. We note that nearly 70% of our measured T_s is between 5 °C and 15 °C, where the discrepancy between modelled and measured $F(t,0) - T_s$ is no greater than 7% (Fig. 6b). Such discrepancy can be attributed to a combination of model underestimation and statistical uncertainty in aggregating chamber measurements (e.g. Lavigne *et al.* 1997).

We estimated the Q_{10} value of the CSO-modelled $F(t,0) - T_s$ relationship in two ways. The first utilizes all the 30-minute runs and the second is based on bin-averages of modelled respiration and soil temperature every 5 °C (Fig. 6a). The Q_{10} values derived from the CSO and the ACES chamber measurements are presented in Table 1. The agreement between the chamber-measured and CSO-modelled Q_{10} is within 6%. The result from the bin-averaged approach is better behaved and is used throughout. Both Q_{10} values derived from ACES chamber measurements and the *CSO* are also well within the range reported in other studies (Raich & Schlesinger 1992; Lavigne *et al.* 1997). However, these Q_{10} estimates are lower than those calculated using data from Andrews &

Table 1 Estimates of Q_{10} and Re_{10} from different experiments at the pine forest stand, Re_{10} is the forest floor respiration at 10 °C. Andrews & Schlesinger's (2001) Q_{10} and Re_{10} are derived from SRC-1 chamber measurements (PP Systems) collected at three plots (FOUR chambers per plot) within the forest, once a month (at noon) from 1996 to 1999. The ACES estimates of Q_{10} and Re_{10} are from 30-minute forest floor flux and soil temperature (T_s) measurements conducted in April–May (60 days) at one plot (14 chambers per plot). The range of values from Andrews & Schlesinger (2001) are due to spatial variability in Q_{10} and Re_{10} among plots

Reference/approach	Q_{10}/Re_{10} using T_s @3 cm	Q_{10}/Re_{10} using T_s @15 cm
Andrews & Schlesinger (2001)	2.3–2.7/2.5–2.6	2.3–2.9/2.5–2.6
Automated Chambers (ACES)	****	1.8/2.1 (April–May 2000, 14 chambers)
CSO Model	****	1.7/2.0 (using 5 °C bin averages)
		1.5/1.9 (using all 30 min runs)

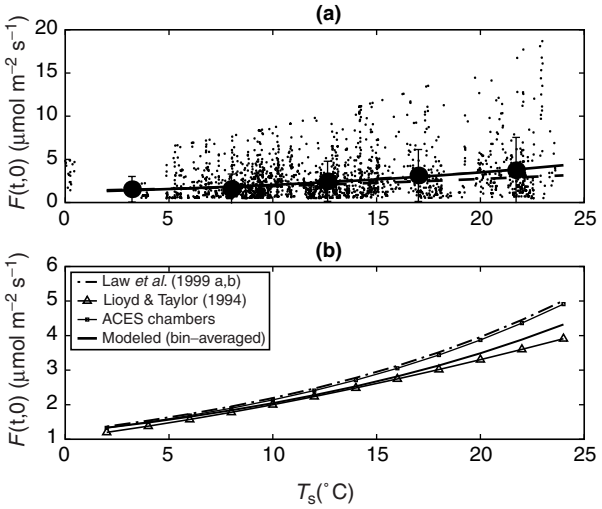

Fig. 6 (a) The 30-minute CSO modelled $F(t,0)$ as a function of measured T_s (dots) at 15 cm below the soil surface. Bin-averaging of $F(t,0)$ along T_s in 5 °C increments is also shown (with one standard deviation). The dashed and solid lines represent the best-fit exponential functions to the raw 30-minute $F(t,0)$ and to the bin-averaged $F(t,0)$, respectively. (b) Comparison between the ACES measured and CSO modelled $F(t,0) - T_s$ curves (bin-averaged). The respiration functions of Law *et al*. (1999a,b) and Lloyd & Taylor (1994) are also presented for reference. For the Lloyd & Taylor (1994) equation, the fitted regression coefficient ($T_0 = 209.58$ K) to the bin-averaged CSO-modelled $F(t,0)$ was used.

Schlesinger (2001) for the same stand. The data of Andrews & Schlesinger (2001) resulted in $Q_{10} = 2.9$ in the vicinity of the flux tower and a mean of 2.5 (when soil temperature measurements at 15 cm are used) for the stand in general (see Table 1). These estimates, higher by more than 30% of all the estimates in Fig. 6, may reflect biases in the measurement system (SRC-1, PP Systems, Haverhill, MA, USA) used by Andrews & Schlesinger (2001). Such discrepancies have been observed in direct field comparisons of the SRC-1, Li-Cor 6400–09 (Li-Cor, Inc.) and ACES (J. Butnor, unpublished data).

Optimized α and plant respiration

The optimized 30-minute α values were averaged over two-month period to obtain mean bi-monthly α values for the entire year. A constraint on α could be derived from daytime $A_{net} - C_i$ curves collected around noon for the upper foliage ($z = 12$ m). Upon fitting these curves to the Farquhar *et al*. (1980) model, the maximum possible α can be determined after R_d and V_{cmax} are computed. Extrapolating the $A_{net} - C_i$ curves to determine R_d from a small magnitude of A_{net} can, in itself, introduce systematic overestimation in R_d because of (i) the linear form of the extrapolating function and (ii) small and unavoidable leaks within gas-analysers tend to increase the value of R_d (Villar *et al*. 1995; Amthor 2000). Based on the sunlit leaf-level $A_{net} - C_i$ measurements and a linear extrapolation for R_d, we found as expected that the mean $\alpha = 0.025$ is larger than the CSO-optimized $\alpha(= 0.012)$ by about 50%, for the same range in temperature in which the $A_{net} - C_i$ curves were collected. We explored a quadratic extrapolation with the following constraints at the CO_2 compensation point (Γ),

$$C_i = \Gamma, \begin{cases} A_{net} = 0 \\ \dfrac{dA_{net}}{dC_i} = V'_{c\,max}, \end{cases}$$

and at $C_i = 0, \frac{dA_{net}}{dC_i} = 0$, where V'_{cmax} is V_{cmax} computed with all kinetic corrections. The fundamental difference between linear and quadratic extrapolations is the slope condition at $C_i = 0$, which assumes R_d independent of C_i for small C_i in the quadratic form. With this quadratic extrapolation, we calculated R_d that is 50% smaller than the linearly extrapolated R_d (Fig. 7) thereby reducing α from 0.025 to 0.0125. The latter α is in excellent agreement with the CSO-computed α, and is in accordance with reported physiological repression of respiration by leaf carbohydrates (Azcon-Bieto 1983; Villar *et al*. 1995). Both the quadratic interpolation for R_d and the *CSO* calculation produced estimates of α within the range of reported values of 0.011–0.015 (e.g. Farquhar *et al*. 1980; Collatz *et al*. 1991).

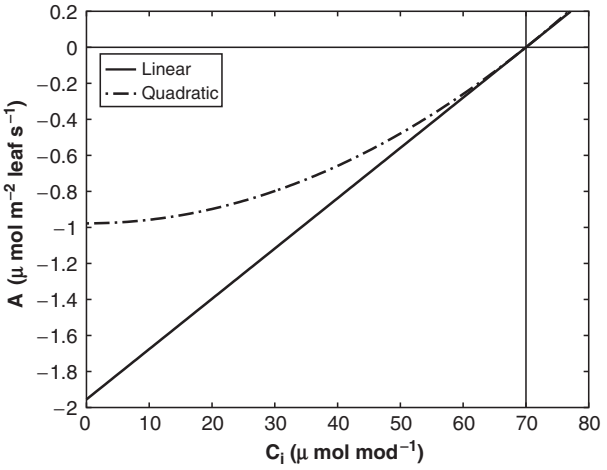

Fig. 7 Estimation of dark respiration (R_d) by extrapolating daytime $A_{net} - C_i$. The solid line is linear extrapolation leading to $\alpha \approx 0.025$. The dotted line is a quadratic extrapolation leading to $\alpha \approx 0.0125$ that is consistent with the CSO-modelled α. The quadratic extrapolation includes repression of respiration by carbohydrates at very low C_i.

Seasonal variation of modelled plant and forest floor respiration

To summarize, we show the relative contribution of CSO-modelled plant and forest floor respiration to the total ecosystem respiration in Fig. 8a–d along with time-matching primary driving variables for different times of the year. The modelled $F(t,0)$ increased with mean soil temperature (Fig. 8c), reaching a near maximum rate of $3.8\,\mu mol\,m^{-2}\,s^{-1}$ in mid-summer (see Fig. 8a). The modelled plant respiration has a similar pattern, and also peaked in mid-summer with a maximum rate $3.1\,\mu mol\,m^{-2}\,s^{-1}$ as a result of the high leaf area density (see Fig. 8d) and high plant tissue temperature. Figure 8b shows the ratio of modelled $F(t,0)/R_E$ in 1999 for different times of the year. This ratio varied from 0.82 to 0.56 from winter to summer, suggesting that the contribution of plant respiration to total ecosystem respiration is much less in the winter when both air temperatures and the leaf area density are low. These model results suggest that estimates of $F(t,0)/R_E$ derived from short field campaigns (even up to 2 months) should not be extrapolated to annual ratios.

Implications for annual ecosystem carbon balance

Based on the CSO-modelled $F(t,0) - T_s$ relationship, mean α values and measured daytime covariance fluxes, the major components of the annual carbon balance of the pine forest ecosystem can be quantified. To estimate daytime net CO_2 exchange, we regressed measured CO_2 fluxes with photosynthetically active photon flux density

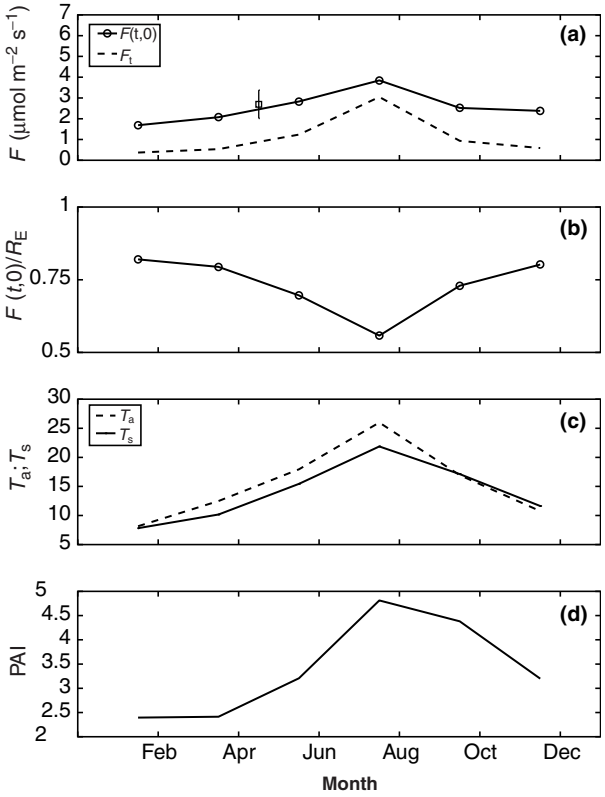

Fig. 8 Seasonal variation of (a) modelled $F(t,0)$ and F_f, and (b) modelled ratio of $F(t,0)/R_E$. For reference, we also show measured T_a and T_s in (c), and measured plant area index (PAI) in (d). For comparison, the ensemble-averaged $F(t,0)$ from chamber measurement is also shown in (a) with one standard deviation.

(*PPFD*) measurements using a nonlinear $F(t,h) - PPFD$ response curve (Landsberg 1986; Ruimy *et al*. 1995; Clark *et al*. 1999; Law *et al*. 1999a), given by:

$$F(t,h) = \frac{\alpha_p\ PPFD F_{sat}}{\alpha_p\ PPFD + F_{sat}} - R_0$$

For this simple analysis, it is assumed that forest carbon assimilation is principally driven by light only with no other limitations (temperature, vapour pressure deficit, drought stress, etc.) explicitly considered. We employ this analysis here only for the purposes of comparing net C assimilation with other forest sites because light interception and radiation use are major determinants of forest productivity (Jarvis & Leverenz 1982; Ruimy *et al*. 1995). The estimated mean apparent quantum yield (α_p), net CO_2 flux at light saturation (F_{sat}), and the mean net CO_2 flux at $PPFD = 0$ (R_0) are all close to the values reported by Clark *et al*. (1999) for a 24-year-old Florida slash pine forest of a similar leaf area index and height (see Table 2). The $F(t,h) - PPFD$ curve is shown in Fig. 9, and the regressed coefficients are compared in Table 2 with the Florida slash pine stand. The $F(t,h) - PPFD$

equation was combined with continuous *PPFD* and other meteorological measurements to yield a net carbon gain of 1342 g C m^{-2} year^{-1}, which is within 10% of the mean value reported by Clark *et al*. (1999).

Using equation 14 and measured soil temperature, $F(t,0)$ was estimated to be 989 g C m^{-2} year^{-1}, well within the range of temperate coniferous forest reported by Raich & Schlesinger (1992). DeLucia *et al*.'s (1999) study at this site reported a soil efflux as 1066 $\pm$ 46 and 928 $\pm$ 9 g C m^{-2} year^{-1} in 1997 and 1998, respectively, consistent with the CSO estimates. Based on the chamber-measured respiration-temperature curve of Fig. 6 (parameters in Table 1), $F(t,0) = 1063$ g C m^{-2} year^{-1}, only 8% higher than the CSO modelled $F(t,0)$.

Combining modelled α, measured plant area density and temperature-adjusted V_{cmax}, F_f was estimated to be 214 g C m^{-2} year^{-1}, slightly greater than the combined foliage and woody respiration reported by Law *et al*. (1999b) for a stand with a lower leaf area density than the loblolly pine ecosystem. The annual NEE of the loblolly pine forest, estimated as the difference between

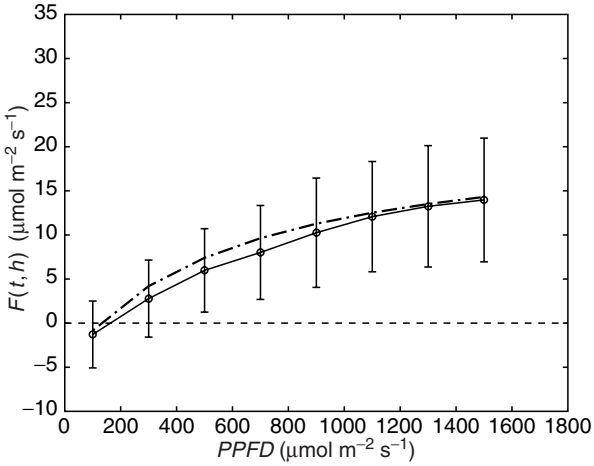

Fig. 9 The whole-ecosystem light response (i.e. $F(t,h) - PPFD$ relationship) derived from the eddy covariance measured $F(t,h)$ at $z/h = 1.1$ (○ with one standard deviation) for the *Pinus taeda* ecosystem. For reference, the $F(t,h) - PPFD$ curve for *Pinus elliotii* reported in Clark *et al*. (1999) is also shown (dot-dashed line).

Table 2 Comparisons of study site characteristics, $F(t,h)$ and coefficients in $F(t,h) - PPFD$ curve between two south-east pine ecosystems. The data for the North Carolina site are for 1999 (also see DeLucia *et al*. 1999 and Ellsworth 2000)

Study site	North Carolina Loblolly pine forest	Florida Slash pine forest
Location	36°2′ N, 79°8′ W	29°44′ N, 82°9′ W
Vegetation type	17-year-old *Pinus taeda L.*	24-year-old (in 1996) *Pinus elliotii* var. *elliotii*
Mean canopy height (m)	14 $\pm$ 0.5 (in 1998)	19.2 $\pm$ 1.0 (in 1996)
Maximum leaf area index	5.0	6.5
Minimum leaf area index	2.4	3.7
Site index at 25 years old	16 m	15 m
Long-term mean air temperature (°C)		
Winter	7.6	14
Summer	27.2	27
Long-term mean annual rainfall (mm)	1154	1332
α_p	0.029	0.044
F_{sat} (μmol m^{-2} s^{-1})	31.2	26.5
R_0 (μmol m^{-2} s^{-1})	3.9	4.6
Ecosystem light compensation point (μmol m^{-2} s^{-1})	156	125
Total daytime net $F(t, h)$ exchange (g C m^{-2} year^{-1})	1342	1529 (1996) 1416 (1997)
Total plant respiration (g C m^{-2} year^{-1})	214	******
Total forest floor respiration (g C m^{-2} year^{-1})	989	1400^{+} (1995–96)
Total night time $F(t,h)$ release (g C m^{-2} year^{-1})	737	789 (1996) 808 (1997)
NEE (g C m^{-2} year^{-1})	1342 − 737 = 605	740 (1996) 608 (1997)
GPP (g C m^{-2} year^{-1})	214 + 989 + 605 = 1808	> 2008

$^{+}$ Estimated by Moncrieff & Fang (1999) from chamber measurements and model simulations

daytime CO_2 gains and night time CO_2 release, was $605\,g\,C\,m^{-2}\,year^{-1}$, also similar to that of the Florida slash pine forest. More importantly, this estimate ($605\,g\,C\,m^{-2}\,year^{-1}$) is also very close to the NEE estimated by the eddy covariance measurements corrected for mean u_* with no gap-filling ($630\,g\,C\,m^{-2}\,year^{-1}$).

With these estimates of R_E and NEE, the estimated GPP $= R_E +$ NEE is $1800\,g\,C\,m^{-2}\,year^{-1}$ for 1999. For the purpose of this study, we define GPP to be carbon assimilation by photosynthesis ignoring photorespiration (Schulze *et al*. 2000). To contrast this estimate with other independent GPP estimates, we consider the measured net primary production (NPP) along with the proposed NPP/GPP of ≈ 0.47 from Waring *et al*. (1998). Based on this ratio and an NPP $\approx 800\,g\,C\,m^{-2}\,year^{-1}$ reported by DeLucia *et al*. (1999) for this pine forest, GPP $\approx 1702\,g\,C\,m^{-2}\,year^{-1}$, within 6% of the GPP determined from measured NEE and CSO-modelled R_E (see Table 3).

Another independent check on the forest GPP can be derived from the ratio of autotrophic respiration (R_A) to net photosynthesis ($A_n =$ GPP). Using isotopic carbon labelling, Andrews *et al*. (1999) estimated the root contribution to be 55% of $F(t,0)$. Combined with our estimate of $F(t,0) \approx 989\,g\,C\,m^{-2}\,year^{-1}$, this yields a contribution by root respiration (R_R) of $544\,g\,C\,m^{-2}\,year^{-1}$. When combined with the above-ground respiration ($\approx F_f = 214\,g\,C\,m^{-2}\,year^{-1}$), $R_A \approx F_f + R_R \approx 758\,g\,C\,m^{-2}\,year^{-1}$. Based on our estimate of GPP, $R_A/GPP \approx 0.42$, which is well within the range of ratios reported by Ryan *et al*. (1994) for pine forests (0.33–0.63, with a mean $= 0.49$; see Table 3). Additionally, we consider the heterotrophic respiration R_H estimated from 45% of $F(t,0)$ as in Andrews *et al*. (1999) and the independently measured root turnover (TO_R) and litter turnover (TO_L) reported by DeLucia *et al*. (1999). Given the measurement uncertainty in these terms, the agreement between estimated R_H ($\approx 445\,g\,C\,m^{-2}\,year^{-1}$) and measured $TO_R + TO_L$ ($\approx 400\,g\,C\,m^{-2}\,year^{-1}$) is remarkably good ($< 10\%$) as shown by the summary results in Table 3.

As a final test, the net photosynthesis A_n can be estimated from a simple Fick's law formulation

$$A_n = g_c C_a \left[1 - \frac{C_i}{C_a}\right]$$

where, g_c is the bulk canopy conductance, directly estimated from sapflux measurements as described in Ewers *et al*. (1999) and Oren *et al*. (1998, 1999), C_i and C_a are the internal and atmospheric CO_2 concentrations, respectively. Using the approach of Lai *et al*. (2000a), the vertically averaged C_i/C_a equals 0.70 for the entire stand. The latter estimate is well within the range of the isotopic carbon analysis reported by Ellsworth (2000) and Katul *et al*. (2000b) for which $C_i/C_a = 0.66$ for sunlit and 0.76 for shaded foliage, respectively. The mean annual sapflux estimated g_c of $70\,mmol/m^2\ s^{-1}$ and $C_a = 370\,\mu mol\ mol^{-1}$, leading to an estimate of A_n (= GPP, as per Schulze *et al*. 2000) of $1825\,g\,C\,m^{-2}\,year^{-1}$for 1999, which is in excellent agreement with the CSO model calculations.

Having demonstrated the consistency between our NEE measurements and modelled $F(t,0)$ with a variety of experiments and literature data, we note that our estimated GPP (*c*. $1800\,g\,C\,m^{-2}\,year^{-1}$) is much larger (*c*. 25%) than the modelled GPP (*c*. 1200–$1300\,g\,C\,m^{-2}\,year^{-1}$) reported in Luo *et al*. (2001) for this pine ecosystem. In Luo *et al*. (2001), a multilevel photosynthesis model (MAESTRA) with an empirical parameterization of stomatal resistance, calibrated with porometry measurements collected at 12 m height, was used to estimate GPP. According to Luo *et al*. (2001), the MAESTRA model calculations reproduced measured NEE by the covariance system. Given that the MAESTRA model

Table 3 Comparison between ecosystem respiration components as modelled by CSO and estimated from published experiments. The units for respiration and GPP are in $g\,C\,m^{-2}\,year^{-1}$

Ecosystem Component	CSO Model	Literature Estimates
GPP	1800	1700 derived from measured NPP = 800 by DeLucia *et al*. (1999) and estimated NPP/GPP = 0.47 by Waring *et al*. (1998).
Forest Floor Respiration	989	928 from DeLucia *et al*. (1999)
Total Root Respiration (R_R)	544	$= 0.55 \times 989$, the 55% is from Andrews *et al*. (1999)
Autotrophic Respiration (R_A)	758	$= 544 + 214$; the 214 is from CSO modelled plant respiration
R_A/GPP	0.42	R_A/GPP $\approx$ 0.33–0.63 reported by Ryan *et al*. (1994) for pine forests (mean = 0.49)
Heterotrophic Respiration (R_H)	445	$= 0.45 \times 989$; the 45% is from Andrews *et al*. (1999) Measured litter turnover = 300 (DeLucia *et al*. 1999) Measured root turnover = 100 (DeLucia *et al*. 1999) Hence, estimated $R_H = 400$ (for 1998 measurements)

reproduced measured NEE (*c.* 630 g C m^{-2} year^{-1}), the model calculations must have underestimated R_E. For instance, combining the measured NEE with measured forest floor respiration from DeLucia *et al*. (1999) (*c.* 928 g C m^{-2} year^{-1} in 1998) results in a GPP of at least 1558 g C m^{-2} year^{-1} without accounting for plant respiration (*c.* 200 g C m^{-2} year^{-1} based on the CSO model calculations). Furthermore, a GPP of 1200 g C m^{-2} year^{-1} and a measured NPP of 800 g C m^{-2} year^{-1} (DeLucia *et al*. 1999) produce a ratio of NPP/GPP = 0.66, 40% higher than the ratio reported by Waring *et al*. (1998), in contrast to good agreement with the results based on the CSO model. Thus the *CSO* model combined with simple photosynthesis formulations as well as the mass-balance of this forest suggest GPP values between 1800 and 2000 g C m^{-2} year^{-1}.

Conclusions

This study proposed a method to estimate components of ecosystem respiration from readily available CO_2 concentration profile measurements. Applying this method to a pine forest in North Carolina, we demonstrated the following:

1. For nocturnal conditions and close to the canopy–atmosphere interface, $\frac{T_L u_*}{h}$ was < 0.3 and sensitive to variations in atmospheric stability h/L. However, $\frac{T_L u_*}{h}$ did not vary appreciably within the canopy (< 20%), at least when assuming $T_L \approx T_w$.
2. Unlike $\frac{T_L u_*}{h}$, σ_w/u_* remained nearly a constant (= 1.1) for a wide range of h/L evaluated at the canopy top. This constant ratio of σ_w/u_* is consistent with a recent study by Leuning (2000) and perhaps suggests that modelling σ_w/u_* for nocturnal conditions may be simpler than unstable conditions.
3. The second-order closure model of Wilson & Shaw (1977) successfully reproduced the measured vertical variation of σ_w/u^* for a wide range of h/L conditions.
4. The combination of LNF and the proposed optimization scheme, termed CSO, reproduced well ecosystem respiration measured with the covariance system under conditions of large u_*. The modelled forest-floor respiration $F(t,0)$ by the CSO approach was in close agreement with the chamber measurements when the night-time CO_2 fluxes are described as a function of soil temperature.
5. Using ecosystem respiration modelled based on the CSO and daytime net CO_2 exchange measured with eddy covariance, we estimated GPP = 1800 g C m^{-2} year^{-1} and NEE = 605 g C m^{-2} year^{-1} for this temperate loblolly pine forest. The ratio of measured NPP to modelled GPP (= 0.44) is close to the general ratio (= 0.47) reported by Waring *et al*. (1998). Furthermore, the modelled plant and forest floor respiration are consistent with measured litter and root turnover rates reported by DeLucia *et al*. (1999), and with isotopic analysis of root : microbial respiration reported in Andrews *et al*. (1999).

The broader implications of this study, when combined with the recent NEE measurements reported in Clark *et al*. (1999) from a Florida slash pine forest ecosystem, is that young (15- to 25-year-old) south-eastern pine forests appear to be among the largest atmospheric terrestrial carbon sinks when compared to other flux sites with published NEE data in Europe and North America (e.g. Wofsy *et al*. 1993; Hollinger *et al*. 1994; Greco & Baldocchi 1996; Valentini *et al*. 2000). These two pine forests along with the *Picea sitchensis* conifer plantation in Valentini *et al*. (2000) exhibit GPP values from 1800 to 2000 g C m^{-2} year^{-1}. Warm temperate conifers at an age close to crown closure are likely to be among the most productive forest ecosystems because their leaf area index is close to maximum and the growing season is very long (Ellsworth 2000), assuring an efficient absorption of photosynthetically active radiation. In addition, according to Waring & Schlesinger (1985), the amount of non-photosynthetic biomass is not very large at this stage of stand developments, assuring limited carbon consumption in respiration.

Acknowledgements

The authors thank Yavor Parashkevov and Andrew Palmiotti for their help during the experiment, the Duke Forest staff for maintaining facilities, and Keith Lewin and John Nagy for their assistance in the CO_2/H_2O multiport design and setup. This project was funded, in part, by the National Science Foundation (NSF-BIR 95–12333 and EAR-9805395), and the US Department of Energy (DOE) through the FACE-FACTS project under contract DE-FG05–95ER62083, and through the National Institute for Global Environmental Change, South-east Regional Center at the University of Alabama, Tuscaloosa (DOE cooperative agreement DE-FC030–90ER61010).

References

Abdella K, McFarlane N (1997) A new second-order turbulence closure scheme for the planetary boundary layer. *Journal of Atmospheric Science*, **54**, 1850–1867.

Amthor J (2000) Direct effect of elevated CO_2 on nocturnal in situ leaf respiration in nine temperate tree species is small. *Tree Physiology*, **20**, 139–144.

Andren A (1990) Evaluation of a turbulence closure scheme suitable for air pollution applications. *Journal of Applied Meteorology*, **29**, 224–239.

Andrews JA, Harrison KG, Matemala R, Schlesinger WH (1999) Separation of root respiration from total soil respiration using ^{13}C labeling during Free-Air-CO_2 Enrichment (FACE). *Soil Science Society of the American Journal*, **63**, 1429–1435.

Andrews JA, Schlesinger WH (2001) Soil CO_2 dynamics in a temperate forest with experimental CO_2 enrichment. *Global Biogeochemical Cycles* **15**, 149–162.

Ayotte KW, Finnigan JJ, Raupach MR (1999) A second-order closure for neutrally stratified vegetative canopy flows. *Boundary-Layer Meteorology*, **90**, 189–216.

Azcon-Bieto J (1983) Inhibition of photosynthesis by carbohydrates in wheat leaves *Triticum aestivum*. *Plant Physiology*, **73**, 681–686.

Baldocchi DD, Valentini R, Running S, Oechel W, Dahlman R (1996) Strategies for measuring and modelling carbon dioxide and water vapour fluxes over terrestrial ecosystems. *Global Change Biology*, **2**, 159–168.

Baldocchi DD, Vogel CA, Hall B (1997) Seasonal variation of carbon dioxide exchange rates above and below a boreal jack pine forest. *Agricultural and Forest Meteorology*, **83**, 147–170.

Black TA, Den Hartog G, Neumann HH *et al.* (1996) Annual cycles of water vapour and carbon dioxide fluxes in and above a boreal aspen forest. *Global Change Biology*, **2**, 219–229.

de Bruin HAR, Kohsiek W, Van Den Hurk BJJM (1993) A verification of some methods to determine the fluxes of momentum, sensible heat, and water vapor using standard deviation and structure parameter of scalar meteorological quantities. *Boundary-Layer Meteorology*, **63**, 231–257.

Campbell GS, Norman JM (1998) *An Introduction to Environmental Biophysics*. Springer-Verlag, NY, pp. 240.

Canuto VM, Minotti F, Ronchi C, Ypma RM, Zeman O (1994) Second-order closure PBL model with new third-order moments: comparison with LES data. *Journal of Atmospheric Science*, **51**, 1605–1618.

Clark KL, Gholz HL, Moncrieff JB, Cropley F, Loescher HW (1999) Environmental controls over net exchanges of carbon dioxide from contrasting Florida ecosystems. *Ecological Applications*, **9**, 936–948.

Collatz GJ, Ball JT, Grivet C, Berry JA (1991) Physiological and environmental regulation of stomatal conductance, photosynthesis and transpiration: a model that includes a laminar boundary layer. *Agricultural and Forest Meteorology*, **54**, 107–136.

Corrsin S (1974) Limitations of gradient transport models in random walks and in turbulence. *Advances in Geophysics*, **18A**, 25–60.

Deardorff JW (1972) Theoretical expression for the countergradient vertical heat flux. *Journal of Geophysics Research*, **77**, 5900–5904.

Deardorff JW (1978) Closure of second and third moment rate equations for diffusion in homogeneous turbulence. *Physics of Fluids*, **21**, 525–530.

DeLucia EH, Hamilton JG, Naidu SL *et al.* (1999) Net primary production of a forest ecosystem with experimental CO_2 enrichment. *Science*, **284**, 1177–1179.

DeLucia EH, Thomas RB (2000) Photosynthetic responses to CO_2 enrichment of four hardwood species in a forest understory. *Oecologia*, **122**, 11–19.

Denmead OT (1995) Novel meteorological methods for measuring trace gas fluxes. *Philosophical Transactions of the Royal Society of London A*, **351**, 383–396.

Denmead OT, Bradley EF (1985) Flux-gradient relationships in a forest canopy. In: *The Forest–Atmosphere Interaction* (eds Hutchison BA, Hicks BB), pp. 421–442. D. Reidel Publishing, MA, USA.

Denmead OT, Raupach MR (1993) Methods of measuring atmospheric gas transport in agricultural and forest system. In: *Agricultural Ecosystem Effects on Trace Gases and Global Climate Change* (eds Duxbury JM, Harper LA, Mosier AR, Rolston DE), American Society of Agronomy, Madison.

Donaldson C, Du P (1973) Construction of a dynamic model for the production of atmospheric turbulence and the dispersion of atmospheric pollutants. In: Workshop on Micrometeorology, American Meteorological Society, pp. 313–392.

Ellsworth DS (1999) CO_2 Enrichment in a maturing pine forest: are CO_2 exchange and water status in the canopy affected? *Plant, Cell, Environment*, **22**, 461–472.

Ellsworth DS (2000) Seasonal CO_2 assimilation and stomatal limitations in a *Pinus taeda* canopy. *Tree Physiology*, **20**, 435–445.

Ewers BE, Oren R, Albaugh TJ, Dougherty PM (1999) Carry-over effects of long term water and nutrient supply on short term water use in *Pinus taeda* trees and stands. *Ecological Applications*, **9**, 513–525.

Falge E, Baldocchi D, Olson R *et al.* (2000) Gap filling strategies for defensible annual sums of net ecosystem exchange. *Agricultural and Forest Meteorology*, **107** (1), 43–69.

Fan S-M, Goulden ML, Munger JW *et al.* (1995) Environmental controls on the photosynthesis and respiration of a boreal lichen woodland a growing season of whole-ecosystem exchange measurements by eddy correlation. *Oecologia*, **102**, 443–452.

Fang C, Moncrieff JB (1996) An improved dynamic chamber technique for measuring CO_2 efflux from the surface of soil. *Functional Ecology*, **10**, 297–305.

Farquhar GD, Von Caemmerer S, Berry JA (1980) A biochemical model of photosynthetic CO_2 assimilation in leaves of C_3 species. *Planta*, **149**, 78–90.

Finnigan JJ (1985) Turbulent transport in flexible plant canopies. In: *The Forest–Atmosphere Interaction* (eds Hutchison BA, Hicks BB), pp. 443–480. D. Reidel Publishing, MA, USA.

Goulden ML, Munger JW, Fan S-M, Daube BC, Wofsy SC (1996) Measurements of carbon sequestration by long-term eddy covariance: methods and a critical evaluation of accuracy. *Global Change Biology*, **2**, 169–182.

Grace J, Malhi Y, Lloyd J, McIntyre J, Miranda AC, Meir P, Miranda HS (1996) The use of eddy covariance to infer the net carbon dioxide uptake of Brazilian rain forest. *Global Change Biology*, **2**, 209–217.

Greco S, Baldocchi DD (1996) Seasonal variations of CO_2 and water vapour exchange rates over a temperate deciduous forest. *Global Change Biology*, **2**, 183–197.

Gu LH (1998) Comments on 'A practical method for relating scalar concentrations to sources distributions in vegetation canopies' by M. R. Raupach. *Boundary-Layer Meteorology*, **87**, 515–524.

Hollinger DY, Kelliher FM, Byers JN, Hunt JE, McSeveny TM, Weir PL (1994) Carbon dioxide exchange between an undisturbed old-growth temperate forest and the atmosphere. *Ecology*, **75**, 134–150.

Jarvis PG, Leverenz JW (1982) Productivity of temperate, deciduous and evergreen forests. In: *Physiological Plant Ecology IV. Encyclopedia of Plant Physiology, New Series* (eds Lange OL,

Nobel PS, Osmond CB, Ziegler H), pp. 233–280. Springer-Verlag, Berlin.

Kaimal JC, Finnigan JJ (1994) *Atmospheric Boundary Layer Flows: Their Structure and Measurements*. Oxford University Press, pp. 289.

Kaimal JC, Gaynor JE (1991) Another look at sonic thermometry. *Boundary-Layer Meteorology*, **56**, 401–410.

Kaiser J (1998) Climate change – new network aims to take the world's CO_2 pulse source. *Science*, **281**, 506–507.

Katul GG, Albertson JD (1998) An investigation of higher order closure models for a forested canopy. *Boundary-Layer Meteorology*, **89**, 47–74.

Katul GG, Albertson JD (1999) Modeling CO_2 sources, sinks, and fluxes within a forest canopy. *Journal of Geophysics Research*, **104**, 6081–6091.

Katul GG, Chang WH (1999) Principal length scales in second-order closure models for canopy turbulence. *Journal of Applied Meteorology*, **38**, 1631–1643.

Katul GG, Ellsworth DS, Lai C-T (2000b) Modelling assimilation and intercellular CO_2 from measured conductance: a synthesis of approaches. *Plant, Cell, Environment*, **23**, 1313–1328.

Katul GG, Hsieh CI, Kuhn G, Ellsworth DS, Nie D (1997b) The turbulent eddy motion at the forest–atmosphere interface. *Journal of Geophysics Research*, **102**, 13409–13421.

Katul GG, Leuning R, Kim J, Denmead OT, Miyata A, Harazono Y (2000a) Estimating CO_2 source/sink distributions within a rice canopy using higher-order closure models. *Boundary-Layer Meteorology*, **98**, 103–125.

Katul GG, Oren R, Ellsworth DS, Hsieh CI, Phillips N, Lewin K (1997a) A Lagrangian dispersion model for predicting CO_2 sources, sinks, and fluxes in a uniform loblolly pine (*Pinus taeda L.*) stand. *Journal of Geophysics Research*, **102**, 9309–9321.

Lai C-T, Katul GG, Ellsoworth DS, Oren R (2000b) Modelling vegetation-atmosphere CO_2 exchange by a coupled Eulerian-Lagrangian approach. *Boundary-Layer Meteorology*, **95**, 91–122.

Lai C-T, Katul GG, Oren R, Ellsworth DS, Schäfer K (2000a) Modeling CO_2 and water vapor turbulent flux distribution within a forest canopy. *Journal of Geophysics Research*, **105**, 26333–26351.

Landsberg JJ (1986) *Physiological Ecology of Forest Production*. Academic Press, London, pp. 198.

Lavigne MB, Ryan MG, Anderson DE *et al.* (1997) Comparing nocturnal eddy covariance measurements to estimates of ecosystem respiration made by scaling chamber measurements at six coniferous boreal sites. *Journal of Geophysics Research*, **102**, 28977–28985.

Law BE, Baldocchi DD, Anthoni PM (1999a) Below-canopy and soil CO_2 fluxes in a ponderosa pine forest. *Agricultural and Forest Meteorology*, **94**, 171–188.

Law BE, Ryan MG, Anthoni PM (1999b) Seasonal and annual respiration of a ponderosa pine ecosystem. *Global Change Biology*, **5**, 169–182.

Leuning R (2000) Estimation of scalar source/sink distributions in plant canopies using Lagrangian dispersion analysis: corrections for atmospheric stability and comparison with a multilayer canopy model. *Boundary-Layer Meteorology*, **96**, 293–314.

Leuning R, Denmead OT, Miyata A, Kim J (2000) Source/sink distributions of heat, water vapor, carbon dioxide, and methane in a rice canopy estimated using Lagrangian dispersion analysis. *Agricultural and Forest Meteorology*, **103**, 233–249.

Leuning R, Judd MJ (1996) The relative merits of open- and closed-path analyzers for measurement of eddy fluxes. *Global Change Biology*, **2**, 241–253.

Lindroth A, Grelle A, Morén A-S (1998) Long-term measurements of boreal forest carbon balance reveal large temperature sensitivity. *Global Change Biology*, **4**, 443–450.

Lloyd J, Taylor JA (1994) On the temperature dependence of soil respiration. *Functional Ecology*, **8**, 315–323.

Luo Y, Medlyn B, Hui D, Ellsworth D, Reynolds J, Katul G, *Ecological Applications*, 11, 235–252.

Maier CA, Kress LW (2000) Soil CO_2 evolution and root respiration in 11 year-old loblolly pine (*Pinus taeda*) plantations as affected by moisture and nutrient availability. *Canadian Journal of Forest Research*, **30**, 347–359.

Massman WJ (2000) A simple method for estimating frequency response corrections for eddy covariance systems. *Agricultural and Forest Meteorology*, **104**, 185–198.

Massman WJ, Weil JC (1999) An analytical one dimensional second-order closure model of turbulence statistics and the Lagrangian time scale within and above plant canopies of arbitrary structure. *Boundary-Layer Meteorology*, **91**, 81–107.

Mellor G (1973) Analytic prediction of the properties of stratified planetary boundary layer. *Journal of Atmospheric Science*, **30**, 1061–1069.

Mellor GL, Yamada T (1974) A hierarchy of turbulence closure models for planetary boundary layers. *Journal of Atmospheric Science*, **31**, 1791–1806.

Moncrieff JB, Fang C (1999) A model for soil CO_2 production and transport 2: application to a florida *Pinus elliotte* plantation. *Agricultural and Forest Meteorology*, **95**, 237–256.

Moncrieff JB, Malhi Y, Leuning R (1996) The propagation of errors in long-term measurements of land atmosphere fluxes of carbon and water. *Global Change Biology*, **2**, 231–240.

Naumburg E, Ellsworth DS (2000) Photosynthetic sunfleck utilization potential of understory saplings growing under elevated CO_2 in FACE. *Oecologia*, **122**, 163–174.

Norman JM, Welles J (1983) Radiative transfer in an array of canopies. *Agronomy Journal*, **75**, 481–488.

Oren R, Phillips N, Ewers BE, Pataki DE, Megonigal JP (1999) Responses of sap flux-scaled transpiration to light, vapor pressure deficit, and leaf area reduction in a flooded *Taxodium distichum* L. forest. *Tree Physiology*, **19**, 337–347.

Oren R, Phillips N, Katul G, Ewers BE, Pataki DE (1998) Scaling xylem sap flux and soil water balance and calculating variance: a method for partitioning water flux in forests. *Annals of Forest Science*, **55**, 191–216.

Oren R, Werk KS, Schulze E-D (1986) Relationships between foliage and conducting xylem in *Picea Abies* (L.) Karst. *Tree Physiology*, **1**, 61–69.

Panofsky HA, Dutton JA (1984) *Atmospheric Turbulence: Models and Methods for Engineering Applications*. Wiley-Interscience, New York, pp. 81–173.

Pataki DE, Oren R, Phillips N (1998) Responses of sap flux and stomatal conductance of *Pinus Taeda* L. trees to stepwise reductions in leaf area. *Journal of Experimental Botany*, **49**, 871–878.

Raich JW, Schlesinger WH (1992) The global carbon dioxide flux in soil respiration and its relationship to vegetation and climate. *Tellus*, **44b**, 81–99.

Raupach MR (1988) Canopy transport processes. In: *Flow and Transport in the Natural Environment* (eds Steffen WL, Denmead OT), pp. 95–127. Springer-Verlag, Berlin.

Raupach MR (1989a) A practical Lagrangian method for relating scalar concentrations to source distributions in vegetation canopies. *Quarterly Journal of Royal Meteorological Society*, **115**, 609–632.

Raupach MR (1989b) Applying Lagrangian fluid mechanics to infer scalar source distributions from concentration profiles in plant canopies. *Agricultural and Forest Meteorology*, **47**, 85–108.

Raupach MR (1998) Response to Gu (1998), 'Comments on ''A practical Lagrangian method for relating scalar concentrations and source distributions in plant canopies'' by M. R. Raupach (1989, *Quart. J. Roy Meteorol. Soc.* 115, 609–632)'. *Boundary-Layer Meteorology*, **87**, 525–528.

Raupach MR, Antonia RA, Rajagopalan S (1991) Rough–wall turbulent boundary layers. *Applied Mechanics Review*, **44**, 1–25.

Raupach MR, Denmead OT, Dunin FX (1992) Challenges in linking atmospheric CO_2 concentrations to fluxes at local and regional scales. *Australian Journal of Botany*, **40**, 697–716.

Raupach MR, Shaw RH (1982) Averaging procedures for flow within vegetation canopies. *Boundary-Layer Meteorology*, **22**, 79–90.

Ruimy A, Jarvis PG, Baldocchi DD, Saugier B (1995) CO_2 fluxes over plant canopies and solar radiation: a review. *Advances in in Ecological Research*, **26**, 1–68.

Ryan MG, Linder S, Vose JM, Hubbard RM (1994) Dark respiration of pines. In: *Ecological Bulletins, Volume 43* (eds Gholz HLS, Linder S, McMurtrie RE), pp. 60–63. Munksgaard Publishers, Copenhagen.

Salas JD, Delleur JW, Yevjevich V, Lane WL (1984) *Applied Modeling of Hydrologic Time Series*. Water Resources Publications, Littleton, Colorado, USA, pp. 484.

Schmid HP, Grimmond CSB, Cropley F, Offerle B, Su HB (2000) Measurements of CO_2 and energy fluxes over a mixed hardwood forest in the mid-western United States. *Agricultural and Forest Meteorology*, **103**, 357–374.

Schulze ED, Wirth C, Heimann M (2000) Managing forests after Kyoto. *Science*, **289**, 2058–2059.

Shaw RH (1977) Secondary wind speed maxima inside plant canopies. *Journal of Applied Meteorology*, **16**, 514–521.

Siqueira M, Lai C-T, Katul GG (2000) Estimating scalar sources, sinks, and fluxes in a forest canopy using Lagrangian, Eulerian, and Hybrid inverse models. *Journal of Geophysical Research*, **105**, 29475–29488.

Sreenivasan KR, Tavoularis S, Corrsin S (1982) A test of gradient transport and its generalization. *Turbulent Shear Flow III*. Springer-Verlag, New York, pp. 96–112.

Tennekes H, Lumley JL (1972) *A First Course in Turbulence*. The MIT Press, Cambridge, MA, pp. 278.

Valentini R, Matteucci G, Dolman AJ *et al.* (2000) Respiration as the main determinant of carbon balance in European forests. *Nature*, **404**, 861–864.

Villar R, Held AA, Merino J (1995) Dark leaf respiration in light and darkness of an evergreen and a deciduous plant species. *Plant Physiology*, **107**, 421–427.

Waring RH, Landsberg JJ, Williams M (1998) Net primary production of forests, a constant fraction of gross primary production? *Tree Physiology*, **18**, 129–134.

Waring RH, Schlesinger WH (1985) *Forest Ecosystems*. Academic Press, Orlando, Florida, pp. 340.

Warland JS, Thurtell GW (2000) A Lagrangian solution to the relationship between a distributed source and concentration profile. *Boundary-Layer Meteorology*, **96**, 453–471.

Wilson JD (1988) A second order closure model for flow through vegetation. *Boundary-Layer Meteorology*, **42**, 371–392.

Wilson JD (1989) Turbulent transport within the plant canopy. In: *Estimation of Areal Evapotranspiration*. IAHS Publishers, 177, 43–80.

Wilson NR, Shaw RH (1977) A higher order closure model for canopy flow. *Journal of Applied Meteorology*, **16**, 1198–1205.

Wofsy SC, Goulden ML, Munger JW *et al.* (1993) Net exchange of CO_2 in a mid-latitude forest. *Science*, **260**, 1314–1317.

Wullschleger SD (1993) Biochemical limitations to carbon assimilation in C3 plants – a retrospective analysis of the A/C_i curves from 109 species. *Journal of Experimental Botany*, **44**, 907–920.

Appendix 1: Second Order Closure Model of Wilson & Shaw (1977)

The following is summarized from Katul & Albertson (1998, 1999) and Katul *et al*. (2000a); for completeness, the final mean momentum and Reynolds stress equations are repeated. In order to model the vertical variation in σ_w, the second order closure model of Wilson & Shaw (1977) is used and is briefly described next. Upon time and horizontally averaging the mean momentum and Reynolds stresses equations, and after performing the simplifications of (i) steady-state adiabatic flow, (ii) assuming that the form-drag by the canopy can be modelled as a drag force, (iii) neglecting the viscous drag relative to the form drag, (iv) closing all the triple-velocity products by a gradient–diffusion approximation (Donaldson & Du 1973; Mellor 1973; Mellor & Yamada 1974; Shaw 1977; Wilson & Shaw 1977; Wilson 1988; Wilson 1989; Andren 1990; Canuto *et al*. 1994; Abdella & McFarlane 1997), (v) modelling the pressure-velocity gradients based on return-to-isotropy principles, (vi) assuming the viscous dissipation is isotropic and dependent on the local turbulence intensity (Mellor 1973), and (vii) assuming horizontal homogeneity, the second-order closure model of Wilson & Shaw (1977) reduces to:

$$\textit{Mean Momentum}: \quad 0 = -\frac{d\overline{u'w'}}{dz} - C_d a(z)\overline{u}^2$$

$$\textit{shear stress}: \quad 0 = -\overline{w'^2}\frac{d\,\overline{u}}{dz} + 2\frac{d}{dz}\left[q\lambda_1\frac{d\overline{u'w'}}{dz}\right] - \frac{q\overline{u'w'}}{3\lambda_2} + C_w q^2\frac{d\,\overline{u}}{dz}$$

$$\textit{Logitudinal Variance}: \quad 0 = -2\overline{u'w'}\frac{d\,\overline{u}}{dz} + \frac{d}{dz} + \left[q\lambda_1\frac{\overline{du'^2}}{dz}\right] + 2C_d a(z)\overline{u}^3 - \frac{q}{3\lambda_2}\left[\overline{u'^2} - \frac{q^2}{3}\right] - \frac{2}{3}\frac{q^2}{\lambda_3}$$

$$\textit{Lateral Variance}: \quad 0 = \frac{d}{dz}\left[q\lambda_1\frac{d\overline{v'^2}}{dz}\right] - \frac{q}{3\lambda_2}\left[\overline{v'^2} - \frac{q^2}{3}\right] - \frac{2}{3}\frac{q^3}{\lambda_3}$$

$$\textit{Vertical Variance}: \quad 0 = \frac{d}{dz}\left[3q\lambda_1\frac{d\overline{w'^2}}{dz}\right] - \frac{q}{3\lambda_2}\left[\overline{w'^2} - \frac{q^2}{3}\right] - \frac{2}{3}\frac{q^3}{\lambda_3}$$

where u_i ($u_1 = u$, $u_2 = v$, $u_3 = w$) are the instantaneous velocity components along x_i, x_i ($x_1 = x$, $x_2 = y$, $x_3 = z$) are the longitudinal, lateral, and vertical directions, respectively, $(\bar{.})$ denotes both time and horizontal averaging (Raupach & Shaw 1982; Raupach *et al*. 1991), and primes denote departures from the temporal averaging operator, $q = \sqrt{\overline{u_i'u_i'}}$ is a characteristic turbulent velocity, λ_1, λ_2 and λ_3 are characteristic length scales for the triple-velocity correlation, the pressure-velocity gradient correlation, and viscous dissipation, respectively (Katul & Chang 1999), κ ($= 0.4$) is Von Karman's constant, C_d is the foliage drag coefficient, γ is an empirical constant, and c_1, c_2, c_3, and C_w are closure constants that can be determined such that the flow conditions well above the canopy reproduce established atmospheric surface layer similarity relations. With estimates of these five constants (c_1, c_2, c_3, C_w and γ), the five ordinary differential equations listed above can be solved for the five flow variables $\overline{u}, \overline{u'w'}, \overline{u'^2}, \overline{v'^2}, \overline{w'^2}$ if appropriate boundary conditions are specified. The flow boundary conditions are assumed to approach the theoretical values of neutral atmospheric surface layer similarity (Panofsky & Dutton 1984) well above the canopy ($z/h > 2$), and zero gradients for all second moments, as well as zero mean velocity at the forest floor. Table 4 summarizes the closure constants used in WS77.

Table 4 The closure constants c_1, c_2, c_3, C_w and γ used in the WS77. Their estimation is discussed in Katul & Albertson (1998) and Katul & Chang (1999)

Closure constant	Remarks
$c_1 = 0.302$	Estimated by matching the WS77 equations, in the absence of flux divergences, to established similarity relations, namely:
$c_2 = 2.313$	$\frac{\sigma_u}{u_*} = 2.4$
$c_3 = 24.296$	$\frac{\sigma_v}{u_*} = 1.9$
$C_w = 0.099$	$\frac{\sigma_w}{u_*} = 1.25$
$\gamma = 0.07$	
$C_d = 0.25$	and that the mixing length is $\kappa(z-d)$, where $\kappa = 0.4$ and d is the height of zero-plane displacement

Appendix 2: Sensitivity Analysis of T_L profile

The results of CSO in Fig. 5 were derived by assuming a vertically constant T_L profile inside the canopy with a correction for atmospheric stability. We repeated the optimization using the three plausible T_L schemes described in the section 'Velocity statistics of nocturnal conditions' to assess how sensitive modelled $F(t,h)$ and $F(t,0)$ are to such an assumption. As shown in Table 5, based on $\frac{T_L u_*}{h} = 0.3$, the model over-predicted $F(t,h)$ and $F(t,0)$ by a factor of 5 and 3, respectively. It clearly shows that such T_L profile is not reasonable for nocturnal conditions. Our calculation improved significantly after T_L was corrected for stability, with case 2 and 3 providing comparable results.

Table 5 Comparisons between modelled to measured ratios of $F(t,h)$ and $F(t,0)$ for the 3 different T_L profiles on annual time scales

Case	$\frac{T_L u_*}{h}$	$F(t,h)$	$F(t,0)$
1	0.3	5.0	3.0
2	f_ϕ; where $f_\phi = \phi_1\left[\frac{h}{L}\right] = \exp(-0.0695x^2 - 0.6454x - 3.8516)$, $x = \ln\left[\frac{h}{L}\right]$	1.2	0.92
3	$f_\phi - 0.155(z_c - 1)$; where $\begin{cases} \frac{z_c = 0.4}{z_c = z/h} & \frac{if\ z/h < 0.4}{if\ z/h \geq 0.4} \end{cases}$	1.37	0.96